

ICF10098OR

Experimental Validation of T^* Integral

Albert S. Kobayashi* and Satya N. Atluri**

*University of Washington, Department of Mechanical Engineering,
Seattle, WA 98195-2600, USA

** University of California, Center for Aeronautical Research and Education,
Los Angeles, CA 90095-1597, USA

T^* integral, which includes J integral as a special case, is shown to be a material property suitable for characterizing crack propagation in thin 2024-T3 aluminum sheets. The T^* resistance curve, which was generated through stable crack growth tests of single edge-notched (SEN) and central notched (CN) specimens, were used to predict curved crack growth and crack link-up of in-line multiple cracks. T^* integral for rapid crack growth reached a maximum value at the terminal crack velocity.

Key Words: Ductile fracture, fracture resistance curve, stable and rapid crack growth, curved crack growth.

INTRODUCTION

The T^* [1], which is a path dependent integral based on incremental theory of plasticity, circumvents much of the difficulties encountered by the J -integral as shown by Brust et. al. [2]. Recently, the author and his colleagues [3] used experimental, numerical and hybrid experimental/numerical techniques to demonstrate the utility of the T^* integral in characterizing stable crack growth in thin aluminum fracture specimens. This study was followed by dynamic and curved crack growth and crack coalescence analyses. These results are summarized in the following.

T^* INTEGRAL

The numerical analyses by Brust et. al. [2] showed that the T^* integral in the very vicinity of the crack tip reaches a plateau with crack extension under creep and cyclic loading. In contrast, the local J -integral vanishes with crack growth. This local T^* , which is designated as T^*_{ϵ} is [1]:

$$T^*_{\epsilon} = \int_{\Gamma_{\epsilon}} \left(W n_1 - t_i \frac{\partial u_i}{\partial x_1} \right) d\Gamma \quad (1)$$

where t_i is the surface traction on the contour Γ_{ϵ} , W is the strain energy density and n_1 is the first component of the normal to the curve. Γ_{ϵ} is an arbitrary small contour immediately surrounding the crack tip and more importantly it elongates together with crack extension. T^*_{ϵ} , as defined by Equation (1), is identical in form of the J integral and therefore T^*_{ϵ} coincides with J where the deformation theory of plasticity prevails. In terms of incremental theory of plasticity, T^*_{ϵ} integral at the end of the N th load steps is the sum of ΔT^*_{ϵ} which is the incremental change of T^*_{ϵ} over a load step or

$$T_{\varepsilon}^* = \sum_{\varepsilon}^N \Delta T_{\varepsilon}^* \quad (2a)$$

where

$$\Delta T = \int_{\Gamma_{\varepsilon}} \left[\Delta W n_1 - (t_i + \Delta t_i) \frac{\partial \Delta u_i}{\partial x_1} - \Delta t_i \frac{\partial u_i}{\partial x_1} \right] d\Gamma \quad (2b)$$

The current T_{ε}^* , as defined by Equation (2), is thus dependent on the prior loading history, a property that is essential for elastic-plastic analysis under crack growth. Although such incremental analysis can be routinely conducted by finite element analysis, it is not practical in experimental analysis as the cumulative experimental errors per load step will eventually overwhelm the sought data. Fortunately, Pyo et al [4] have shown, through numerical experiments, that the total T_{ε}^* integral computed directly by using the stresses and strains based on the incremental theory of plasticity, was for practical purpose equal to the summed ΔT_{ε}^* of Equation (2). Thus Equation (1) can be used for crack growth study without the cumbersome incremental procedure provided the states of stress and strain are based on the incremental theory of plasticity. More recently, T_{ε}^* was also studied extensively by Nishioka and his colleagues [5].

ε is governed by the plate thickness for a plane stress state to exist along the integration contour of Γ_{ε} . This distance, ε , is equated to the plate thickness after Narashimhan and Rosakis [6]¹. For a plane strain state, this characteristic distance could be several times the crack tip radius.

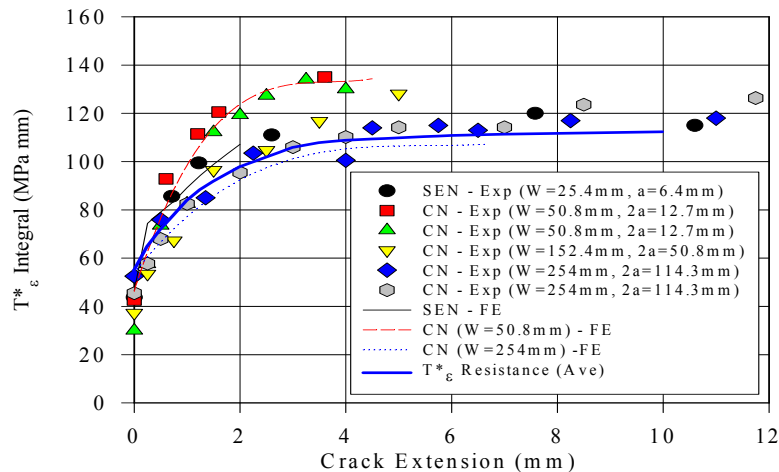
METHOD OF APPROACH

By restricting the integration contour very close to and along the extending crack, Okada and Atluri [7] have shown that the contour integration trailing the crack tip can be neglected by virtue of the closeness of Γ_{ε} to the traction free crack surface. Since the contour integral is now restricted to the frontal portion of Γ_{ε} , the deformation theory of plasticity can now be used to compute the stresses in the loaded portion of Γ_{ε} . The experimental procedure consisted of measuring the two orthogonal displacement fields surrounding a stably growing or a rapidly propagating crack in thin, single edge notched (SEN), central notched (CN) and compact (CT), 2024-T3 aluminum specimens. The strains and stresses, using the equivalent stress-strain and the measured uniaxial stress-strain data of the 2024-T3 sheet, were computed. Finally, Equation (1) was evaluated numerically along the contour, Γ_{ε} .

RESULTS

SEN and CN Specimens

Experimentally determined T_{ε}^* integral data of one SEN specimen and five CN specimens of different cracks lengths with saw cut or fatigued crack tip are shown in Fig. 1. For a contour size of $\Gamma_{\varepsilon} = 1$ mm, the T_{ε}^* data for the 152.4 mm and 254 mm wide specimens are approximately equal. Other than the 50.8 mm wide CN specimens, the experimental T_{ε}^* data of the SEN and CN specimens practically coincide thus suggesting that the T_{ε}^* is a geometry-independent material property of this material. The T_{ε}^* resistance curve represents the average of this data. As shown in Fig. 1, the T_{ε}^* resistance curve rises at the initial stage of crack growth and reaches a constant value during steady crack growth. In contrast, the global J resistance curve, J_R , continually rises with stable crack extension and includes energy from other sources.



¹ The three-dimensional elastic-plastic finite element analysis of a flat crack in plate by Narashimhan and Rosakis [17] showed that the plane stress state prevailed at one half of the plate thickness from the crack tip. Since a 100 percent shear lip is the norm in ductile fracture, the minimum distance, ε , was conservatively picked as the plate thickness.

Fig. 1. SEN and CN experimental T^*_{ϵ} resistance curve ($L_{\epsilon} = 1\text{mm}$)

While the J integral based instability criterion is determined on a global basis, the instability criterion for T^*_{ϵ} integral is locally based. During steady crack growth, the state of stress is in equilibrium and thus the parameter characterizing this phenomenon should be constant. When the driving force exceed the material's resistance, i.e. $T^*_{\epsilon} > T^*_{\epsilon R}$, instability will occur without an additional applied load or a displacement.

For crack growth simulation, a load or displacement was applied as the boundary condition and the crack was propagated when $T^*_{\epsilon} > T^*_{\epsilon R}$. With the prescribed load or displacement held constant, T^*_{ϵ} was evaluated again for the extended crack. If T^*_{ϵ} remained greater than $T^*_{\epsilon R}$, the crack was extended again, and T^*_{ϵ} was re-evaluated. The crack continued to extend until T^*_{ϵ} dropped below $T^*_{\epsilon R}$. Additional load/displacement was applied to the specimen until T^*_{ϵ} was equal to $T^*_{\epsilon R}$ where upon another node was released to extend the crack. This procedure was repeated until no additional load or displacement was required to propagate the crack. At that point, instability was assumed to have occurred. The results identified as "FE" in Fig. 1 show that this simulation compared very well with the experimental data.

Curved Crack Growth

Twenty four biaxial test specimens were fabricated without or with bonded, bonded and riveted and integral pad-up tear straps and tested to failure. The results obtained in six tests, i.e. without tear straps, with bonded, bonded and riveted and machined pad-up tear straps are report in this paper. Figure 2 shows the variation in $T^*_{I\epsilon}$, which corresponds to the mode I contour integral of Equation (1), along the frontal portion of Γ_{ϵ} at various crack tip locations of the curved cracks. The steady state $T^*_{I\epsilon}$ in this study coincides with the corresponding T^*_{ϵ} resistance curve of Fig. 1. The increase in $T^*_{I\epsilon}$ of Experiments B21 and B25, as the crack

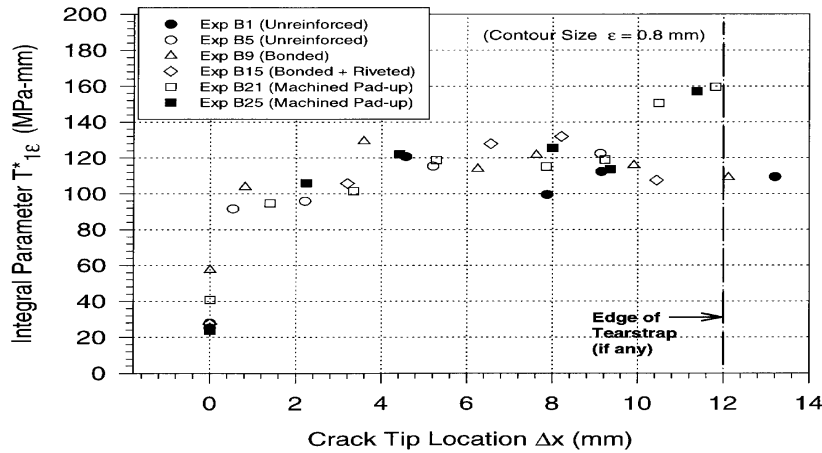


Fig. 2. $T^*_{I\epsilon}$ variation with curved crack growth.

approaches the tear strap, represents the increased resistance to crack growth in these machined pad-up tear straps. Such an increase was not observed in Experiments B9 and B15, thus suggesting that the bonded and bonded-riveted tear straps may not be as effective as the machined pad-up tear straps in resisting curve crack extension. Indeed, the final load at fracture in the machined pad-up tear straps was 30 percent higher than that of the bonded and bonded-riveted tear straps.

$T^*_{2\epsilon}$, which is the mode II equivalent of $T^*_{I\epsilon}$, oscillated about its null value throughout the entire curved crack extension. These results suggest that $T^*_{I\epsilon}$ is the resistance for a locally self-similar crack growth and that the crack curves in the direction of vanishing $T^*_{2\epsilon}$. These results are the elastic-plastic counterpart to the vanishing K_{II} criterion for curved elastic crack growth [8,9]. The experimentally determined value of $T^*_{I\epsilon}$ during stable crack growth is approximately 120 MPa-mm which is 5 percent higher than the T^*_{ϵ} resistance curve in Figure 1.

Crack Link-up

The feasibility of using the T^*_{ϵ} resistance curve of Fig. 1 to predict crack growth and linkup in the presence of multiple site damage (MSD) was tested through a series of MSD experiments. The experimental procedure consisted of determining the T^*_{ϵ} integral experimentally and measuring the crack growth and linkup in MSD2 specimens with two cracks, MSD3 specimens with a center/lead crack approaching two holes with MSD cracks and MSD5 specimens with a center/lead crack and four holes. These specimens were machined from the same Al 2024-T3 clad aluminum sheet of thickness 0.8 mm. All cracks were oriented in the L-T direction and special buckling guides were used to prevent the out-of-plane buckling of the fracture specimen.

Specimens MSD5_08 (ligament = 12.7 mm and $a_{msd} = 2.5$ mm) and MSD5_13 (ligament 20.32 mm $a_{msd} = 2.5$ mm) failed simultaneously with the first crack linkup. The experimental T^*_{ϵ} versus crack extension for both specimens are shown in Figs. 3(a) and (b). In both cases, all the cracks exhibited stable crack growth at T^*_{ϵ} values similar to the CN specimen. Crack tips C and

D extended approximately 3 mm and 1.5 mm prior to linking up. Specimen MSD5_16, which had the same crack configuration as MSD5_08, was subjected to three cyclic loads. At each cycle, the load was increased until crack tip D extended approximately 0.8 mm. The specimen was then unloaded to 10% of the maximum load. Experimental T^*_ϵ was evaluated for each crack extension as the specimen was cyclic loaded. Figure 3(c) shows that T^*_ϵ values under cyclic and monotonic loads are the same during crack growth. Thus the T^*_ϵ generated from a monotonically loaded CN specimen may also be used to characterize low cycle fatigue crack growth.

Dynamic Crack Propagation

Dynamic T^*_ϵ has been previously determined experimentally using the laser caustic method by Nishioka et al in 1991 [10]. In this study [11, 12], dynamic moiré interferometry was used to determine the transient displacement fields perpendicular and parallel to the running crack in 7075-T6 aluminum alloy, single edge notch (SEN) specimen. The SEN specimen was either fatigue precracked or blunt notched for low and high crack velocity tests, respectively. By neglecting the contour integral behind the propagating crack, only a partial near-crack contour at $\epsilon = 2$ mm from the crack was used in the integration process thus simplifying the T^*_ϵ computation. The measured crack tip displacement field was also used to compute the LEFM-based strain energy release rate, G .

Data in Fig. 4 identified as the first series is from Lee, Kokaly and Kobayashi [11] using fatigue precracked specimens and the second series refers to the data from the blunt notched specimens [12]. When plotted in terms of the crack velocity, the combined first and second series of tests, T^*_ϵ increased with increasing crack velocity and eventually leveled off at a terminal velocity of about 300 m/s as shown in Fig. 4. Literature on dynamic fracture show that the LEFM based dynamic strain energy release rate, G_{ID} with respect to crack velocity exhibits a characteristic gamma-shaped curve. The LEFM based G_{ID} for the dynamic fracture tests of 7075-T6 aluminum specimens and the blunt-notched 7075-T6 SEN specimens of Kobayashi and Engstrom [13] did yield this gamma-shaped curve. The LEFM approach results in a terminal velocity, which is insensitive to the variation in the driving force, G_{ID} , while the T^*_ϵ approach, based on elastic-plastic fracture mechanics (EPFM), suggests that the terminal crack velocity is a consequence of the saturation of the dissipated plastic energy.

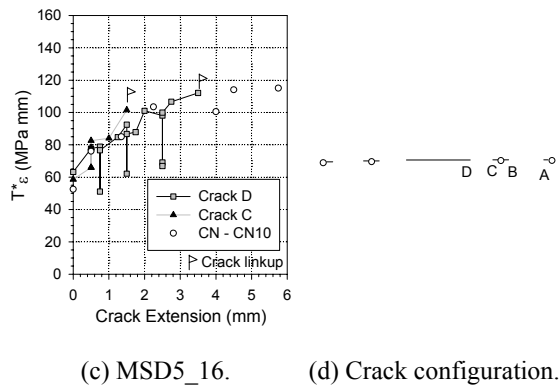
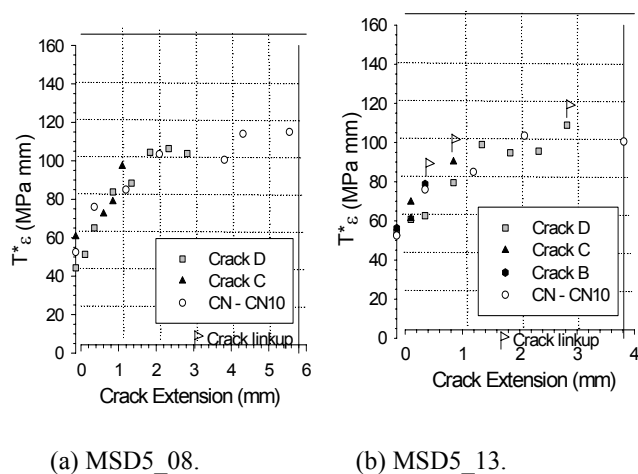


Fig. 3. T^*_ϵ associated with stable crack growth.

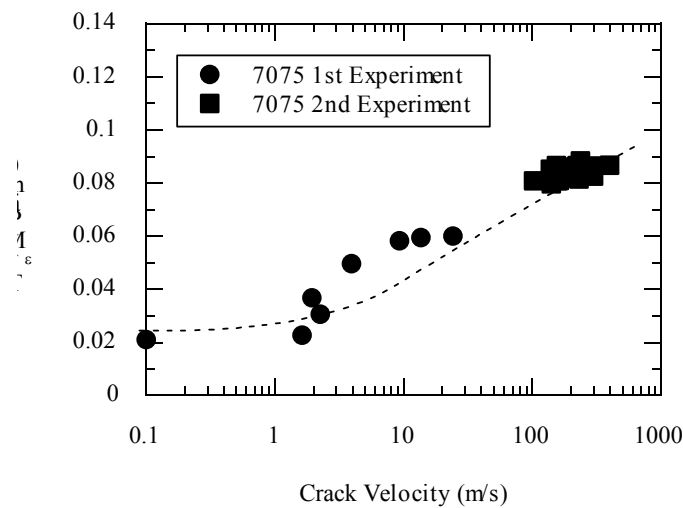


Fig. 4. T^*_{ϵ} versus crack velocity.

CONCLUSIONS

The experimental evidences accumulated over the past six years suggest that T^*_{ϵ} integral is a material property characterizing stable and dynamic crack growth. Specifically:

1. T^*_{ϵ} resistance curve reaches a plateau with static and dynamic crack growth
2. Crack curves in the direction of vanishing $T^*_{2\epsilon}$ and grows with $T^*_{1\epsilon}$ following the T^*_{ϵ} resistance curve.
3. A crack instability criterion based on the T^*_{ϵ} resistance curve was proposed and experimentally verified.
4. Dynamic T^*_{ϵ} value reached a constant value at terminal crack velocity.

ACKNOWLEDGEMENT

This paper summaries the cumulative efforts of the authors' colleagues of the past ten years. In chronological order, they are: Drs. Y. Omori, Pratt and Whitney Company, J. Lee, Republic of Korea Air Force, L. Ma, United Technology Research Center, P. Lam, Orbital Sciences Corporation and M. T. Kokaly, Fatigue Technology, Inc. This research was supported by FAA Grant No. 92-G-005 and ONR Contract N0001489J1276.

REFERENCES

1. Stonesifer, R.C. and Atluri, S.N., On a Study of the (ΔT) and C^* Integrals for Fracture Analysis Under Non-Steady Creep, *Engineering Fracture Mechanics*, Vol. 16 (1982), pp. 769-782.
2. Brust, F.W., Nishioka, T., Atluri, S.N. and Nakagaki, M., Further Studies on Elastic-Plastic Stable Fracture Utilizing the T^* Integral, *Engineering Fracture Mechanics*, Vol. 22 (1985), pp. 1079-1103.
3. Omori, Y., Okada, H., Ma, L., Atluri, S.N. and Kobayashi, A.S., T^*_{ϵ} Integral Under Plane Stress Crack Growth, *Fatigue and Fracture Mechanics, 27th Volume*, ASTM STP 1296 (1997), eds. P.S. Plasik, J.D. Newman, and N.E. Dowling, pp. 61-71.
4. Pyo, C.-R., Okada, H. and Atluri, S.N., An Elastic-Plastic Finite Element Alternating Method for Analyzing Wide Spread Fatigue Damage in Aircraft Structures, *Computational Mechanics*, Vol. 16 (1995), pp. 62-68.
5. Nishioka, T. and Yagami, H., Invariance of the Path Independent T^* Integral in Nonlinear Dynamic Fracture Mechanics, with Respect to the shape of a Finite Process Zone, *Engineering Fracture Mechanics*, Vol. 31 (1988), pp. 481-491.
6. Narasimhan, R. and Rosakis, A.J., Three-Dimensional Effects Near a Crack Tip in a Ductile Three-Point Bend Specimen: Part I—A Numerical Investigation,” *ASME Journal of Applied Mechanics*, Vol. 57 (1990), pp. 607-617.
7. Okada, H. and Atluri, S.N., Further Study on the Characteristics of the T^*_{ϵ} Integral Plane Stress Stable Crack Propagation in Ductile Materials, *Computational Mechanics*, Vol. 23 (1999) pp. 339-352.
8. Cottrell, B. and Rice, J.R., Slightly /curved or Kinked Crack, *International Journal of Fracture*, Vol. 10 (1980), pp. 155-169.
9. Sumi, Y., Nemat-Nasser, S. and Keer, L.M., On the Crack Path Stability in a Finite Body, *Eng'g Fracture Mechanics*, Vol. 22 (1985), pp. 759-771
10. Nishioka, T., Sakai, K., Murakami, T. Matsuo, S. and Sakakura, K., Measurement of Nonlinear Fracture Parameter T Integral under Impact Loading Using Laser Caustic Method, *Transactions of 11th International Conference on Structure Mechanics in Reactor Technology*, G13/1 (1991), Tokyo, pp. 321-326.
11. Lee, J., Kokaly, M.T. and Kobayashi, A.S., Dynamic Ductile Fracture of Aluminum SEN Specimens: An Experimental-numerical Analysis. *International Journal of Fracture*, Vol. 93 (1999), pp. 39-50.
12. Kokaly, M.T., Lee, J. and Kobayashi, A.S., Dynamic Ductile Fracture of 7075-T6 – An Experimental analysis, to be published in the *International Journal of Solids and Structures*.
13. Kobayashi, A.S. and Engstrom, W.L., Transient analysis in fracturing aluminum plates, *Proceedings of 1967 JSME Semi-International Symposium*, JSME (1967), pp. 172-181.